Steel and Composite Structures, *Vol. 30, No. 4 (2019) 393-403*
DOI: https://doi.org/10.12989/scs.2019.30.4.393

Structural efficiency of various strengthening schemes for cold-formed steel beams: Effect of global imperfections

M. Adil Dar [1], N. Subramanian [2], A.R. Dar [*3], Muheeb Majid [3], Mohd Haseeb [3] and Mugees Tahoor [3]

[1] *Department of Civil Engineering, Indian Institute Technology Delhi, New Delhi, India*
[2] *Consulting Engineer, Maryland, USA*
[3] *Department of Civil Engineering, National Institute Technology Srinagar, J&K, India*

(*Received October 22, 2018, Revised February 9, 2019, Accepted February 25, 2019*)

Abstract. Cold-formed steel (CFS) has a great potential to meet the global challenge of fast-track and durable construction. CFS members undergo large buckling instabilities due to their small wall thickness. CFS beams with corrugated webs have shown great resistance towards web buckling under flexure, when compared to the conventional I-sections. However, the magnitude of global imperfections significantly affects the performance of CFS members. This paper presents the first attempt made to experimentally study the effect of global imperfections on the structural efficiency of various strengthening schemes implemented in CFS beams with corrugated webs. Different strengthening schemes were adopted for two types of beams, one with large global imperfections and the other with small imperfections. Strength and stiffness characteristics of the beams were used to evaluate the structural efficiency of the various strengthening schemes adopted. Six tests were performed with simply supported end conditions, under four-point loading conditions. The load vs. mid-span displacement response, failure loads and modes of failure of the test specimens were investigated. The test results would compensate the lack of experimental data in this area of research and would help in developing numerical models for extensive studies for the development of necessary guidelines on the same. Strengthening schemes assisted in enhancing the member performance significantly, both in terms of strength and stiffness. Hence, providing an economic and time saving solution to such practical structural engineering problems.

Keywords: cold-formed steel; experiment; strengthening; beams; imperfections; buckling; capacity

1. Introduction

Cold formed steel (CFS) structures are structural products that are prepared by forming plane sheets of steel at an ambient temperature into different shapes that can be used to satisfy structural and functional requirements (Dubina *et al*. 2012, Hancock 2016, 2001). CFS proves to be an ideal choice in situations where moderate loads and spans make hot-rolled steel shapes with limited sections, uneconomical. Cold rolling process can be employed to produce almost any desired shape within suitable spans. Other primary advantages of CFS include lightness in weight, high strength and stiffness, ease of prefabrication and mass production, more accurate detailing, non-shrinkage and non-creeping at ambient temperatures, uniform quality and fast track construction. CFS members with selective stiffening arrangements perform better than the unstiffened ones in terms of strength, stiffness and economy (Dar *et al*. 2019). The main problem encountered in the light gauge steel is its local buckling. This stability failure occurs well before the material has reached its yield strength (which leaves the section un-utilized to its full capacity), thus limiting the section to reach its full strength potential.

*Corresponding author, Professor,
E-mail: abdulrashid@nitsri.net

However, researchers have addressed this issue by developing innovative sectional profiles like corrugated web with flange plates, which either delays or completely eliminates such stability failures (Kumar and Sukumar 2014, Soliman *et al*. 2013). The wave formation (local buckling) at the early stage of loading in CFS built-up members with large flat-to-width ratio do not prevent the member's strength to resist further loads (Dar *et al*. 2018a, El Aghoury *et al*. 2013). Intermediate ties prove very helpful in delaying the premature buckling in CFS members (Anbarasu and Sukumar 2014). CFS sections with innovative profiles and proper stiffening arrangements delay their premature instabilities (Ammash 2017, Biggs *et al*. 2015, Dar *et al*. 2015a). Adequately designed CFS composite sections prove to be efficient as well as economical, with higher stiffness characteristics (Dar *et al*. 2018b, Valse Ipe *et al*. 2013). Properly designed built-up CFS members show immense potential in development of efficient and economical sections (Serror *et al*. 2017). Innovative tubular webs showed significantly better performance in steel moment resisting frames with typical shallow beams (Saleh *et al*. 2016). The applied forces and the rotational restraint stiffness of the lipped flange (in CFS lipped channels used as compression members) exhibit a linear coupling relationship (Zhou and Jiang 2017). Proper detailing of CFS members ensures their better performance and easy assembling (Kumar and Sahoo 2016, Dundu 2012).

ISSN: 1229-9367 (Print), 1598-6233 (Online)

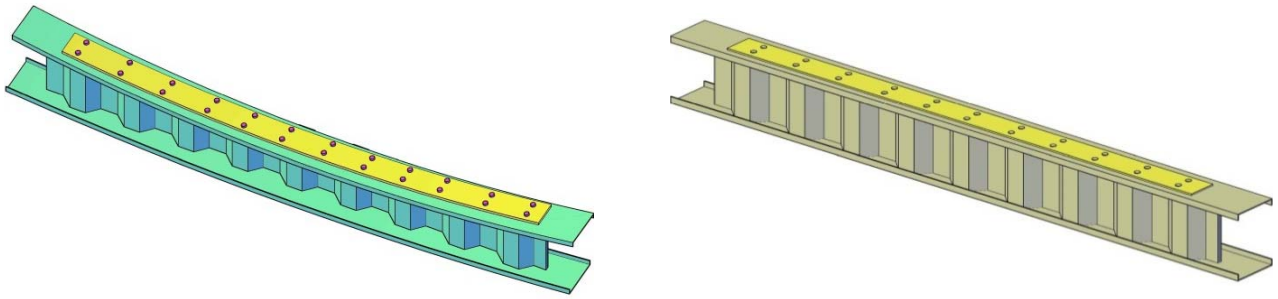

(a) Model A5 (beam with large imperfection) (b) Model A (beam with small imperfection)

Fig. 1 Adoption of global strengthening

CFS straight beams are ideal, but do not exist in reality. Hence, CFS beams are usually associated with varying magnitudes of geometric imperfections that mainly depend on the quality of workmanship. Geometric imperfections affect the buckling behaviour, strength as well as the stiffness performance of CFS members. Ultimate bending capacities of beams with overall slenderness ratios ranging from the short to intermediate levels, are sensitive to the imperfect shape that comprise of compression flange local buckling for long beams. The Lateral–torsional buckling is the most sensitive buckling mode (Gendy and Hanna 2015). Physical imperfections lead to the residual stresses that appear in steel structural profiles and plates during the manufacturing process and if no technique is used to alleviate these residual stresses, they unavoidably remain on the profiles or plates (Martins *et al*. 2017).

The magnitude and nature of distress in distressed structures needs to be evaluated both in terms of strength and stiffness characteristics, to take a call on the feasibility of restoration. Strengthening is preferable, particularly when new construction is not feasible and dismantling can prove unsuitable both in terms of cost and time. The remedial measures adopted in a distressed roof truss improved its strength and stiffness substantially. However, the performance of the remedial measures adopted was affected by the completeness of the truss action and the nature of loads the truss member was subjected to (Dar *et al*. 2017).

In this study, for the first time, an attempt is made experimentally to study the effect of global imperfections on the structural efficiency of various strengthening schemes on the behaviour of CFS beams with corrugated webs. Different strengthening schemes were adopted for two types of beams, one with large global imperfections and the other with small imperfections, as shown in Fig. 1. Strength and stiffness characteristics of the beams were used to evaluate the structural efficiency of the various strengthening schemes adopted. Six tests were performed with simply supported end conditions, under four-point loading conditions. The load vs. mid-span displacement response, failure loads and modes of failure of the test specimens were investigated. The test results of this investigation will not only fill the gap of lack of experimental data of these CFS beams but also be useful for those conducting numerical studies to check their results and also develop necessary guidelines.

2. Experimental investigation

2.1 Methodolody

Since the objective is to study the effect of global imperfections on the structural efficiency of various strengthening schemes of CFS beams with corrugated webs, it was necessary to set a benchmark of parameters like strength and stiffness. Accordingly, two identical CFS beams with double trapezoidal corrugated webs were fabricated. One of the beams was tested under monotonic concentrated loading to impart a curved profile (sag) to the beam. This beam specimen due to sagged profile will have higher global imperfections, thus will have reduced strength as well as stiffness.

While introducing sag in the curved beam, local buckling of flange occurred at one of the loading points. Thus, local strengthening was needed to prevent failure at that location. Accordingly, local strengthening of the buckled area was carried out, by removing the buckled flange plate, and welding a new plate to the web at the same point. An additional cover plate was bolted over to the flange in the affected area, as a mark of safety and to compensate the losses incurred due to the removal of the damaged portion and residual stresses developed due to welding. Using the concept of shear flow, a particular arrangement of bolts in terms of spacing and configuration was proposed and provided.

After providing local strengthening with the proposed bolt arrangement, the beam was tested and found to fail owing to loss of composite action between the cover plate and the beam. So, both the bolt spacing and arrangement was changed to improve the composite action.

Once the efficiency of the local strengthening was assessed, it was necessary to adopt global strengthening and assess the same. Global strengthening was adopted by providing a hot rolled plate bolted to the compression flange with particular bolt spacing.

After testing the globally strengthened beam specimen, it was observed that the specimen would have performed better, had a closer spacing of bolts been adopted. Hence, the bolt spacing was modified and the modified globally strengthened beam specimen was tested.

After testing the modified globally strengthened beam specimen, the influence of providing a similar hot rolled plate on the tension side was also evaluated. Accordingly,

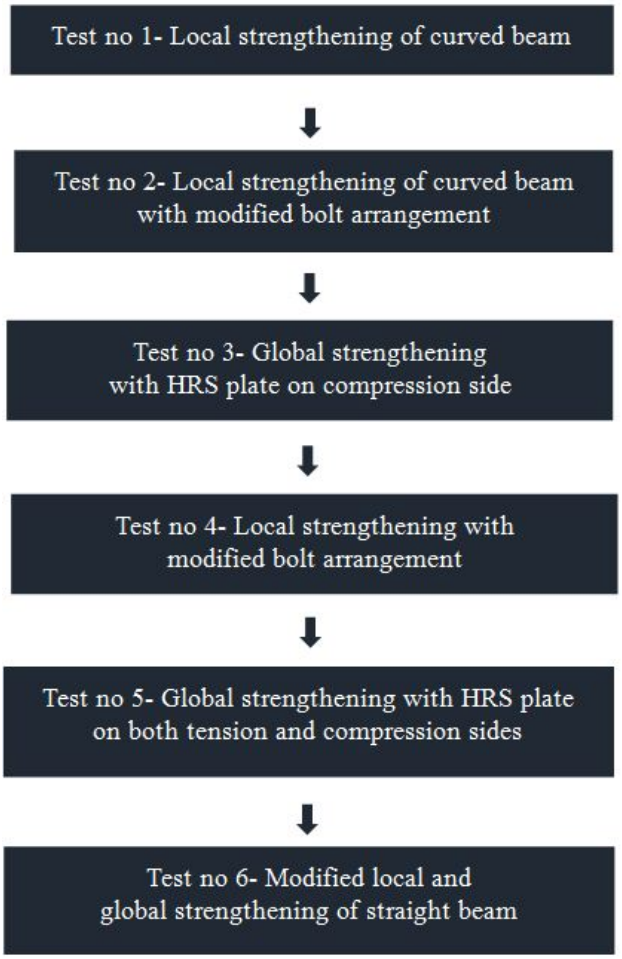

Fig. 2 Scheme of the tests performed

the beam specimen was modified and tested. These led to the testing of a series of distressed CFS beams which were strengthened after each test.

To check the effect of global imperfections on the strengthening, all these global strengthening schemes were implemented to the CFS beam with less global imperfections (the ones that are imparted due to workmanship errors only) also. This would give a comparison of the efficiency of the strengthening schemes with reference to variation in global imperfections. The scheme of these tests is shown in Fig. 2.

2.2 Test specimens details

For achieving the primary objective of this study, two identical CFS beams with double trapezoidal corrugated webs were fabricated. The thicknesses of flange and web are 2 mm and 1.6 mm respectively. Two trapezoidal plates forming the web were connected to each other with bolts of size 5 mm and grade of 4.6 to form a double trapezoidal corrugated web as shown in Fig. 3(a). Flange plates were connected to this web through welded connection as shown in Fig. 3(b). Figs. 3(c) and (d) show the isometric view and sectional view of the CFS double trapezoidal webbed beam. The dimensional details of the CFS double trapezoidal webbed beam specimen are given in Table 1 and Fig. 4. These specimens had less global imperfections, which were of the range of span of beam/1700 and span of beam/1900 in downward and lateral directions respectively.

As mentioned earlier that one of the two CFS double trapezoidal webbed beam specimens was tested under monotonic concentrated loading to impart a curved profile (sag) to the beam. This beam specimen had a global

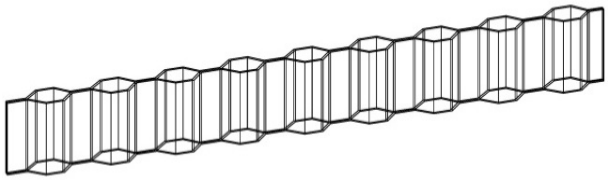

(a) Double trapezoidal corrugated web

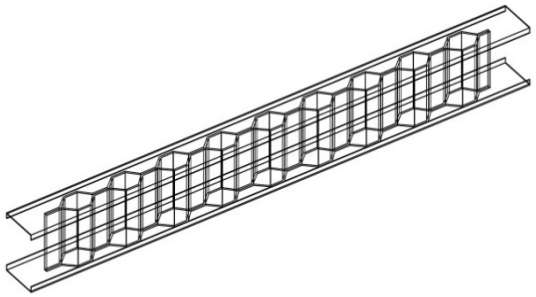

(b) Corresponding beam

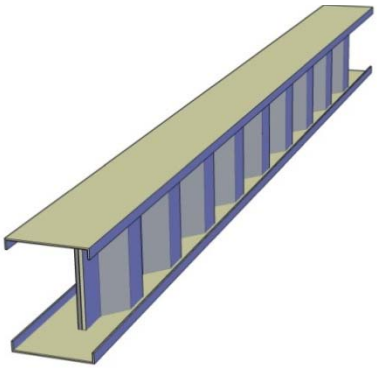

(c) Isometric view of the specimen

(d) Sectional view of the specimen

Fig. 3 Preparation of the CFS double trapezoidal webbed beam

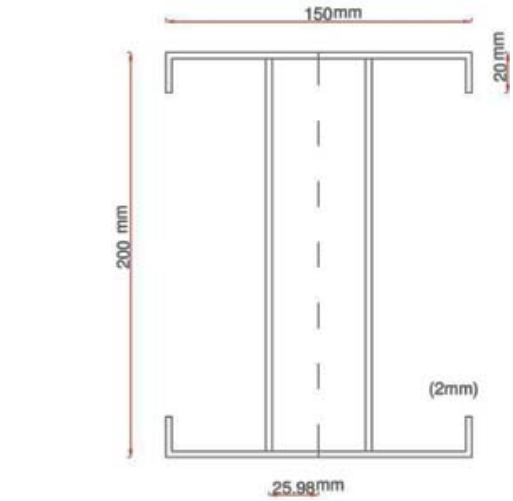

(a) Sectional view

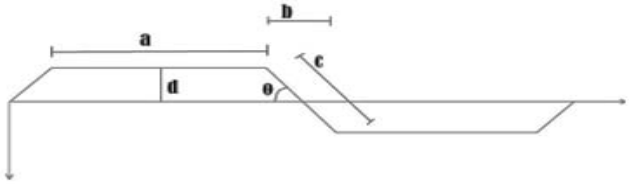

(b) Details of the trapezoidal web

Fig. 4 Dimensional details of the CFS double trapezoidal webbed beam specimen

imperfection of 2.62 mm at the centre. This beam specimen was labelled as Model A1 or curved beam. After each successive test, the curved beam strengthened and was labelled as Model A2, Model A3, Model A4 and Model A5. Finally, the strengthening schemes adopted in Model A5 was adopted in other left out CFS double trapezoidal webbed beam specimen. This specimen with less global imperfection was labelled Model B or Straight beam. Finally, the efficiency of the strengthening schemes adopted in Model A5 and Model B were compared, in order to evaluate the effect of global imperfections on the same.

While introducing sag in one of the two CFS double trapezoidal webbed beam specimens, local buckling of flange occurred at one of the loading points. The length of flange affected by local buckling was 170 m.The strengthening measure proposed for the same was removal of the buckled flange part, and welding of a new plate of same thickness to the web at the same point. An additional cover plate of same thickness and of length 320 mm was bolted over to the flange over the entire flange width in the affected area. The details of local strengthening are given in Table 2 and Fig. 5(a). This specimen will be called as Model A1 for future references.

After loading of Model A1, the bolt arrangement proved to be inadequate. Hence the bolt arrangement was improved (as shown in Table 2 and Fig. 5(b)) and this beam specimen with enhanced bolt arrangement for cover plates will be called Model A2 for future references.

Table 1 Dimensional details of the CFS double trapezoidal webbed beam specimen

Span (m)	Depth (mm)	Breadth (mm)	Lip depth (mm)	Flange thickness (mm)	Web thickness (mm)	a (mm)	b (mm)	c (mm)	d (mm)	θ
2.42	200	150	20	2	1.6	60	30	60	25.98	60^o

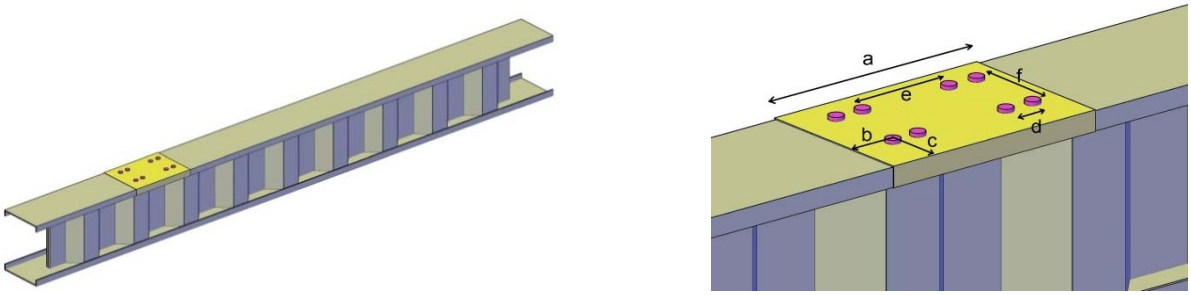

(a) Model A1

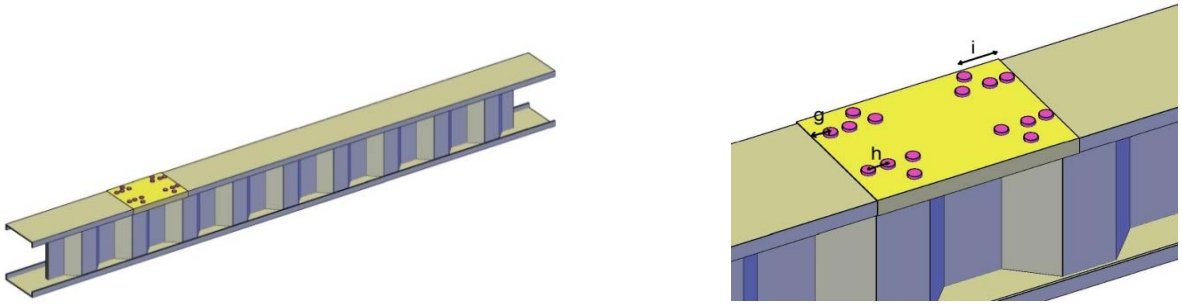

(b) Model A2

Fig. 5 Details of local strengthening schemes adopted

Table 2 Details of local strengthening schemes adopted

Model	a (mm)	b (mm)	c (mm)	d (mm)	e (mm)	f (mm)	g (mm)	h (mm)	i (mm)
Model A1	320	50	45	60	110	90	-	-	-
Model A2	320	50	45	60	110	90	20	40	80

Table 3 Details of global strengthening schemes adopted

Model	Compression plate specifications			Tension plate specifications		
	Thickness (mm)	Width (mm)	Bolt spacing (mm)	Thickness (mm)	Width (mm)	Bolt spacing (mm)
Model A3	6	100	164	-	-	-
Model A4	6	100	82	-	-	-
Model A5	6	100	82	6	100	164
Model B	6	100	82	6	100	164

After assessing the efficiency of local strengthening schemes, it was necessary to evaluate the performance of global strengthening as well. Hence, Model A2 was globally strengthened in the compression zone (compression flange) with hot rolled steel plate of width 100 mm and thickness of 6 mm over the entire length of the CFS beam. Two rows of bolt spacing with a longitudinal spacing of 164 mm was adopted and is given in Table 3. This modified specimen will be called as Model A3 for future references.

During the testing of Model A3, loss of composite action was observed due to inadequate bolt spacing in the longitudinal direction. Hence, the said bolt spacing was modified by decreasing it to 82 mm. This beam specimen with modified spacing will be called Model A4 for future references.

Further, the effect of introducing a similar hot rolled steel cover plate of same specifications in the tension flange of Model A4, with a bolt spacing of 164 mm (because of being on the tension side) needed to be assessed, and was accordingly implemented. This beam specimen with modified spacing will be called Model A5 for future references and is shown in Fig. 1(a).

Since the straight beam specimen (one of the left out CFS double trapezoidal webbed beam specimen) did not suffer from any local buckling (like flange buckling in Model A1), only global strengthening schemes i.e., hot rolled steel plate was bolted to the tension as well as compression flange. This beam specimen will be called Model B for future references and is shown in Fig. 1(b). The details of this model are given in Table 3.

2.3 Material properties

CFS double trapezoidal webbed beam specimens were fabricated from locally available structural steel. To determine the mechanical properties of the steel used for fabrication, tensile coupon tests were conducted. Three coupons were prepared from the centre of the flange in the longitudinal direction. The dimensions of the coupons, as conforming to the Indian Standards (IS1608:2005), were used for material testing. A computerized universal testing machine was used to conduct the tensile tests of the coupons. Since hot-rolled steel was used for strengthening, tensile coupon test was also performed for the same. Stress-Strain curves for CFS is shown in Fig. 6. The relevant material properties of the both the CFS and hot rolled steel obtained from the material testing are given in Table 4.

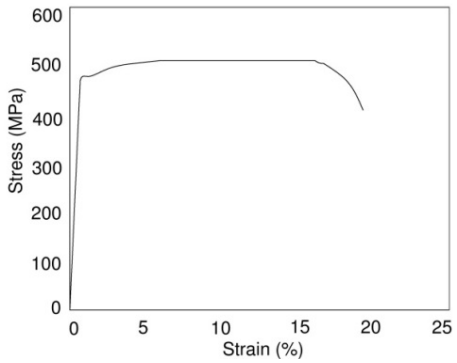

Fig. 6 Stress vs. strain behaviour of CFS steel used

Table 4 Material properties of steel used

Test	f_n (MPa)	E (GPa)	f_y (MPa)	f_u (MPa)	Δ
Cold-formed steel					
1 (2 mm)	350	209	455	510	18
2 (2 mm)	350	207	468	496	20
3 (2 mm)	350	208	454	505	19
Average	350	207	459	504	19
Hot rolled steel					
1	250	214	266	433	26
2	250	212	272	457	23
3	250	210	275	442	26
Average	250	212	271	444	25

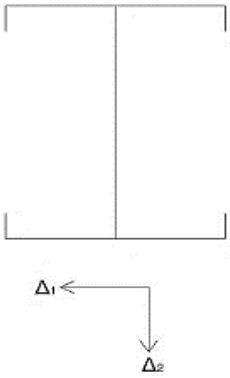

Fig. 7 Direction of global imperfections

Table 5 Magnitude of global imperfections

Specimen	Δ_1/L	Δ_2/L
Model A1	1/1142	1/923
Model A2	1/1091	1/541
Model A3	1/1030	1/202
Model A4	1/995	1/83
Model A5	1/908	1/42
Model B	1/1921	1/1751

2.4 Geometric imperfections

Before testing, the initial geometric imperfections were measured for Model A and Model B. These imperfections were measured near the centre both along longitudinal and transverse directions at the bottom flange web junctions. A calibrated vernier calliper and an optical theodolite were used to obtain the readings at the mid length and near ends of the model. Geometric imperfections for final models i.e. Model A1 and Model B whose strengthened capacity are to be compared were also measured using the same technique. The imperfections measured in models along two orthogonal directions as shown in Fig. 7, are given in the Table 5. For comparison, the magnitude of the maximum and minimum imperfections ranged between 1/2131 to 1/4346 (Dar *et al*. 2019).

2.5 Test setup

Testing of beams was carried out using a reaction frame 500 kN capacity as shown in Fig. 8. The vertical monotonic loading was applied by means of a hydraulic loading jack of 500 kN. Since, the beam specimens were intended to be tested under four-point loading. Accordingly, such an arrangement was simulated by using the spreader beam (I-section ISWB 175) with attachments for rollers placed at 0.7 m apart as shown in Fig. 9. This whole four-point load arrangement had weight of 0.16 KN (approximately). Four bearing stiffeners were used to prevent the web buckling of the beam at loading points and at reaction points. These bearing stiffeners comprised of two hot rolled steel angles ISA 50 × 50 × 5 placed back to back, which were welded to the web of the beam specimens on both sides. Electronic dial gauges with least count of 0.01 mm were used to record the downward displacements. Bearing plates of size 150 mm

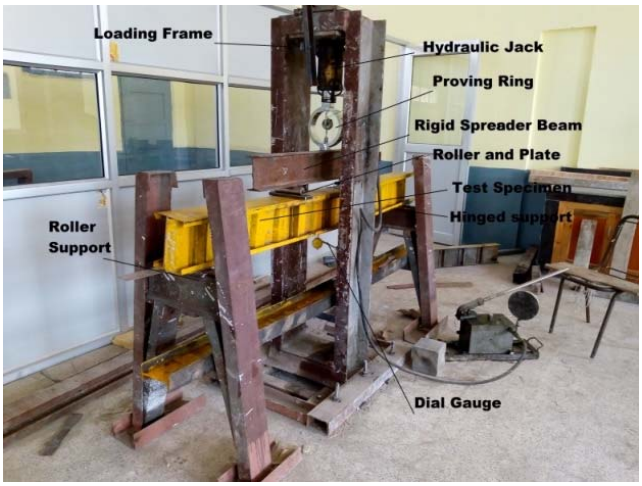

Fig. 8 Test set-up adopted

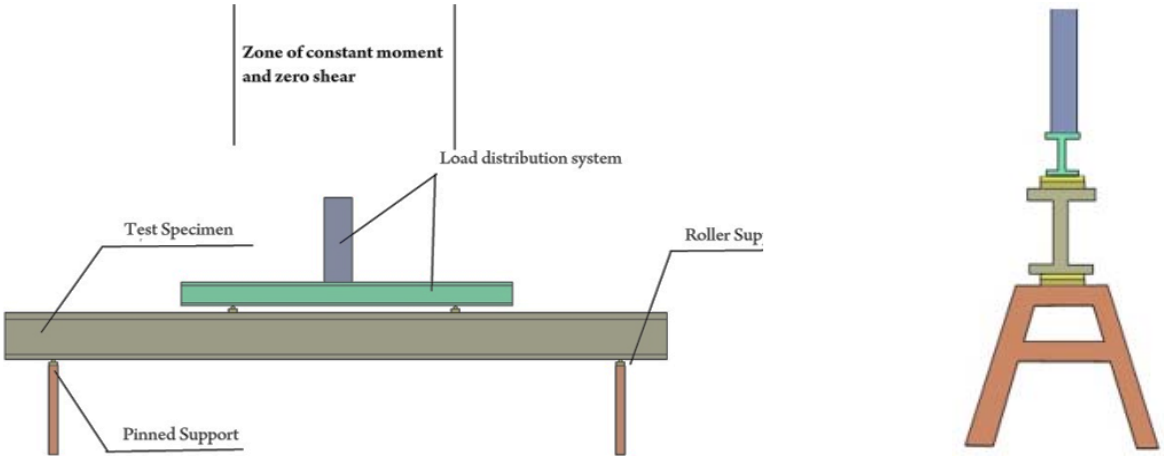

(a) Elevation (b) Cross-section

Fig. 9 Four-point loading arrangement

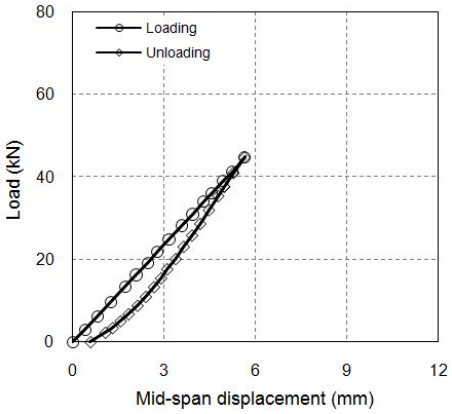

(a) Load vs. mid-span displacement curve

(b) Failure in Model A1

Fig. 10 Test results of specimen A1

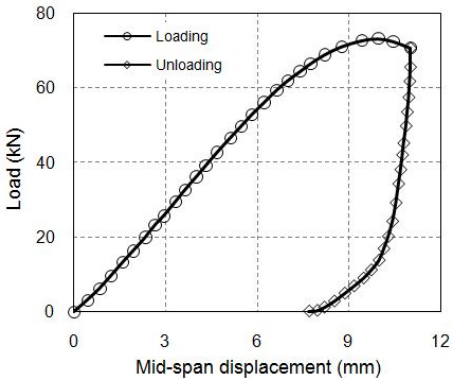

(a) Load vs. mid-span displacement curve

(b) Local flange buckling in Model A2

Fig. 11 Test results of specimen A2

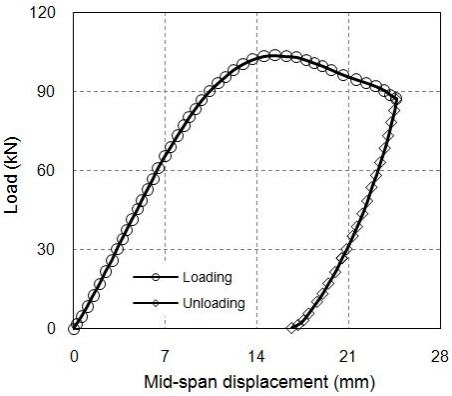

(a) Load vs. mid-span displacement curve

(b) Failure in Model A3

Fig. 12 Test results of specimen A3

× 60 mm × 15 mm were placed under concentrated loading points to prevent punching failure. Four-point loading arrangement was mainly chosen over three-point load arrangement to provide a pure flexure zone in the middle third section of the beam specimen. Further details pertaining to the test set-up can be found elsewhere (Dar *et al*. 2015b).

3. Test results and discussion

Fig. 10(a) shows the load *vs*. mid-span displacement of Model A1. Since the bolt spacing proposed was inadequate. Hence, the beam specimen failed due to loss in composite action (as shown in Fig. 10(b)) at a load of 44.53 kN (i.e., nearly within elastic limit) and corresponding mid-span

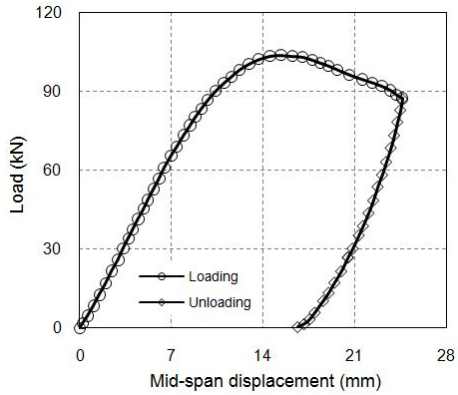

(a) Load vs. mid-span displacement curve

(b) Failure in Model A4

Fig. 13 Test results of specimen A4

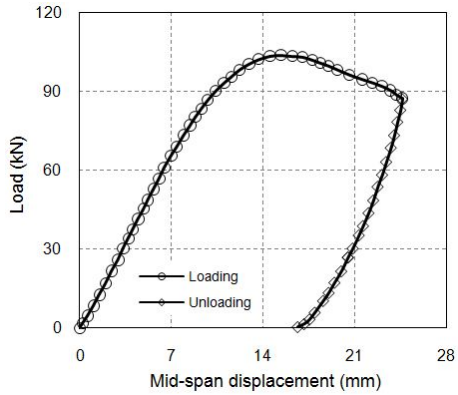

(a) Load vs. mid-span displacement curve

(b) Local web buckling

(c) Lateral torsional buckling

Fig. 14 Test results of specimen A5

displacement of 5.45 mm. The cover plate was detached from the flange which clearly indicated loss in composite action between the cover plate and flange.

Fig. 11(a) shows the load *vs*. mid-span displacement of Model A2. The beam failed at a load of 71.98 kN and corresponding mid-span displacement of 11.06 mm. Local flange buckling at the point of loading (the location where cover plate was attached) was observed and is shown in Fig. 11(b). Smooth increasing trend in the curve (Fig. 11(a)) confirms beam action. Initially the curve behaves linearly. Later, increase in rate of deformation was observed, which is primarily due to initiation of local flange buckling that continues until the maximum load is resisted. After unloading the model, a permanent set of 7.42 mm was observed.

Fig. 12(a) shows the load *vs*. mid-span displacement of Model A3. Model A3 failed at a load of 95.16 KN and a maximum mid-span displacement of 24.97 mm. The beam failed by loss of composite action between the flange and hot rolled plate (as shown in Fig. 12(b)) which was anticipated as the specimen had already yielded. After unloading, a permanent set of 17.14 mm was observed.

Fig. 13(a) shows the load *vs*. mid-span displacement of Model A4. The model failed at a load of 97.6 KN and at a maximum mid-span displacement of 21.1 mm. The failure observed was in the form of flexural yielding and lateral torsional buckling as shown in Fig. 13(b). After unloading, a permanent set of 16.88 mm was observed.

Fig. 14(a) shows the load *vs*. mid-span displacement of Model A5. This model carried a maximum load of 153.55 kN and maximum mid-span displacement of 18.85 mm was observed. The failure occurred by local web buckling and lateral torsional buckling as shown in Figs. 14(b) and (c) respectively. The addition of another hot rolled steel plate on tension flange delayed the local buckling failure. After unloading, a permanent set of 6.83 mm was observed.

Fig. 15(a) shows the load *vs*. mid-span displacement of Model B. The beam carried a maximum load of 208.08 kN and a maximum mid-span displacement of 45.22 mm was observed. Local web buckling along with local flange

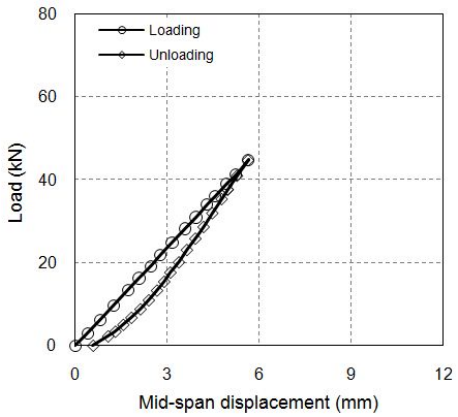

(a) Load vs. mid-span displacement curve

(b) Local web buckling

(c) Local flange buckling

Fig. 15 Test results of specimen B

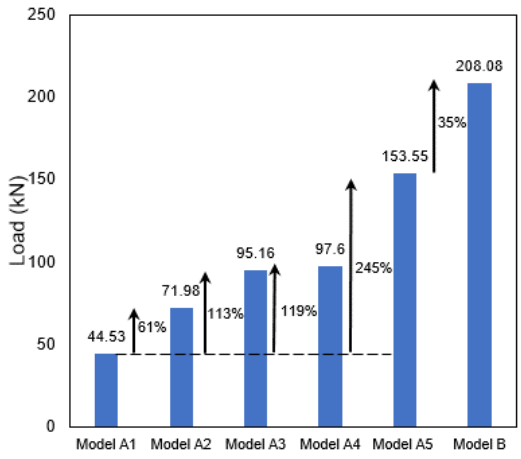

(a) Strength comparison

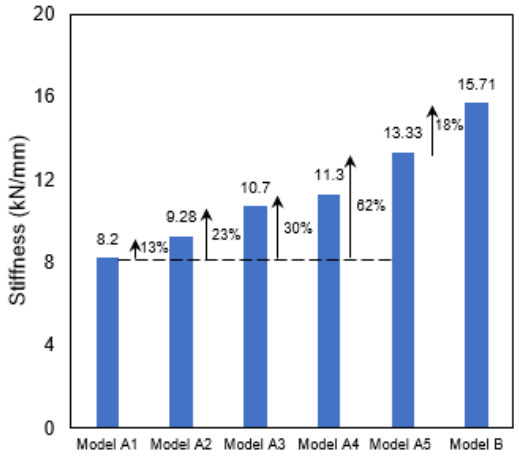

(b) Stiffness comparison

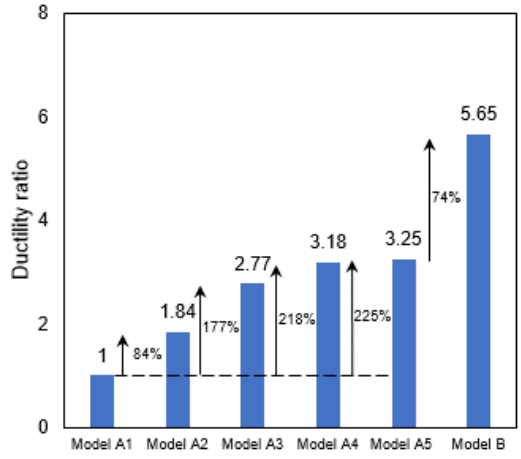

(c) Ductility ratio comparison

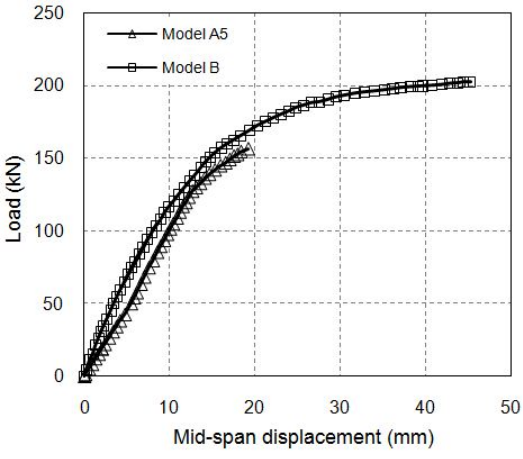

(d) Mid-span displacement comparison

Fig. 16 Comparison of test results

Table 6 Comparison of test results

Model	Failure load (kN)	Maximum mid-span Displacement (mm)	Stiffness (kN/mm)	Increase in strength (%)	Increase in stiffness (%)
Model A1	44.53	5.45	8.2	-	-
Model A2	71.98	11.06	9.28	38.1%	13.2%
Model A3	95.16	24.97	10.7	32.2%	15.3%
Model A4	97.6	21.1	11.3	2.6%	5.6%
Model A5	153.55	18.85	13.33	57.3%	18%
Model B	208.08	45.22	15.71	35.5%	17.9%

buckling in the vicinity of load application was observed as shown in Figs. 15(b) and (c) respectively. Abrupt increase in the rate of deflection can be attributed to local buckling of web in combination with local flange buckling in the vicinity of load applied. After unloading, a permanent set of 28.5 mm was observed.

Fig. 16 and Table 6 presents the comparison of test results with respect to strength, stiffness and ductility ratio. Further, a comparison of load *vs*. mid-span displacement between Model A5 and B is also presented in Fig. 16(d). It was seen that with every strengthening measure adopted, the strength, stiffness as well as ductility ratio improved. However, the strength improvement in Model B over Model A5 was higher (35%) compared to the stiffness improvement (only 18%). Local strengthening schemes in CFS beams with large global imperfections were able to improve the strength nearly by up-to 100%. However, the adoption of global strengthening resulted in the improvement of about 250%. Furthermore, the global strengthening was seen to be dependent upon the magnitude of global imperfections. The improvement was higher in CFS beams with lesser global imperfections. The performance of strengthening will further depend upon the sectional compactness of the CFS section to be strengthened. From serviceability consideration, only global strengthening schemes showed better performance. From ductility consideration, both local as well as global strengthening schemes performed well. While adopting local as well as global strengthening schemes, due consideration must be given to the connection details to ensure proper composite action between the CFS section and the additional steel strip attached for the purpose of strengthening. In the load *vs*. mid-span displacement curve (Fig. 16(b)), the trend followed by Model A5 and Model B was same. However, the maximum mid-span displacement in Model B was larger, but at a much higher loading. The un-factored design strength of the double trapezoidal CFS beam with corrugated web (Model B) as per North American Specifications (AISI S-100) and Indian Standards (IS 801) is 52.27 kN and 48.9 kN respectively. The predictions were slightly un-conservative. The level of un-conservativeness was due to the magnitude of global imperfections.

4. Recommendations

Based on the test results, the following recommendations have been made for CFS beams with corrugated webs:

- Local strengthening should be resorted in CFS beams with large global imperfections, only when the required strength improvement is less than 100%. For much better performance, global strengthening schemes should be adopted. However, the strengthening adopted will depend upon the sectional compactness of the CFS section.
- From serviceability consideration, only global strengthening schemes provide the required performance.
- From ductility consideration, both local as well as global strengthening schemes provide necessary performance. However, global strengthening schemes are preferable.
- While adopting local as well as global strengthening schemes, due consideration must be given to the connection details to ensure proper composite action between the CFS section and the additional steel strip attached for strengthening purpose.

5. Conclusions

Based on experimental investigation carried out to study the effect of global imperfections on the structural efficiency of various strengthening schemes for CFS beams with corrugated webs, following important conclusions were drawn:

- Both local as well as global strengthening schemes improve the strength as well as stiffness characteristics of CFS beams with corrugated webs having large global imperfections. The local strengthening schemes were able to strengthen the curved beam by up to 113% in terms of strength, up to 30% in terms of stiffness and up to 177% in terms of ductility ratio. The improvement of the same characteristics in the curved beam with global strengthening schemes were found to be 245%, 62% and 225% respectively.

- The appreciable improvement in the capacity of strengthened curved CFS beams proves that such strengthening schemes can be used without the need for using new structural members. Thus, the suggested strengthening schemes provide an economic and time saving solution to such real-world problems. The adopted strengthening schemes not only enhanced their load carrying capacity, but also helped to reduce their deflections. Hence, such schemes are useful from the angle of serviceability criteria.
- The improvement in strength, stiffness, and ductility ratio of the globally strengthened CFS straight beam was higher than that of the globally strengthened CFS curved beam. The increase in strength, stiffness and ductility ratio for the former specimen was 35%, 18% and 74% respectively, when compared with the latter one. This proves that residual stresses can cause appreciable reduction in the capacity of a member.
- Bolt spacing and their arrangement plays vital role in providing composite action, particularly for local strengthening.
- Loss of composite action, local flange buckling, local web buckling, and lateral torsional buckling were the modes of failure observed in strengthened curved CFS beams. However, only local flange buckling and local web buckling were observed in the strengthened CFS straight beam.

It has to be noted that the structural behaviour of closed CFS sections may be different from that of open CFS sections. As this study focused only on the response of open CFS sections to the different strengthening schemes, the conclusions are applicable only to these open CFS sections.

References

AISI S-100 (2016), North American Specification for the Design of Cold-formed Steel Structural Members; AISI Standard, Washington, DC, USA.

Ammash, H.K. (2017), "Shape optimization of innovation cold-formed steel columns under uniaxial compressive loading", *Jordan J. Civil Eng.*, **11**(3), 473-489.

Anbarasu, M. and Sukumar, S. (2014), "Influence of spacers on ultimate strength of intermediate length thin walled columns", *Steel Compos. Struct., Int. J.*, **16**(4), 437-454.

Biggs, K.A., Ramseyer, C., Ree, S. and Kang, T.H.K. (2015), "Experimental testing of cold-formed built-up members in pure compression", *Steel Compos. Struct., Int. J.*, **18**(6), 1331-1351

Dar, M.A., Dar, A.R., Yusuf, M. and Raju, J. (2015a), "Experimental study on innovative sections for cold formed steel beams, *Steel Compos. Struct., Int. J.*, **19**(6), 1599-1610.

Dar, M.A., Subramanian, N., Dar, A.R. and Raju, J. (2015b), "Experimental investigations on the structural behaviour of a distressed bridge", *Struct. Eng. Mech., Int. J.*, **56**(4), 695-705.

Dar, M.A., Subramanian, N., Dar, A.R. and Raju, J. (2017), "Rehabilitation of a distressed steel roof truss – A study", *Struct. Eng. Mech., Int. J.*, **62**(5), 567-576.

Dar, M.A., Sahoo, D.R., Pulikkal, S. and Jain, A.K. (2018a), "Behaviour of laced built-up cold-formed steel columns: Experimental investigation and numerical validation", *Thin-Wall. Struct.*, **132**, 398-409.

Dar, M.A., Subramanian, N., Dar, A.R., Anbarasu, M. and Lim, J.B.P. (2018b), "Structural performance of cold-formed steel composite beams", *Steel Compos. Struct., Int. J.*, **27**(5), 545-554.

Dar, M.A., Subramanian, N., Dar, A.R., Anbarasu, M., Lim, J.B.P. and Mir, A. (2019), "Behaviour of partly stiffened cold-formed steel built-up beams: Experimental investigation and numerical validation", *Adv. Struct. Eng.*, **22**(1), 172-186.

Dubina, D. and Ungureanu, V. (2002), "Effect of imperfections on numerical simulation of instability behaviour of cold-formed steel members", *Thin Wall. Struct.*, **40**, 239-262.

Dubina, D., Ungureanu, V. and Landolfo, R. (2012), *Design of Cold-Formed Steel Structures*, (First Edition), Wiley, New York.

Dundu, M. (2012), "Base connections of single cold-formed steel portal frames", *J. Constr. Steel Res.*, **78**, 38-44.

El Aghoury, M.A., Salem, A.H., Hanna, M.T. and Amoush, E.A. (2013), "Strength of cold formed battened columns subjected to eccentric axial compressive force", *J. Constr. Steel Res.*, **113**, 58-70.

Gendy, B.L. and Hanna, M.T. (2015), "Effect of geometric imperfections on the ultimate moment capacity of cold-formed sigma-shape sections", *HBRC Journal*, **13**(2), 163-170.

Hancock, G.M. (2001), *Cold-Formed Steel Designing and Analysis*, Marcel Dekker, Sydney, Australia.

Hancock, G.J. (2016), "Cold-formed steel structures, research review", *Adv. Struct. Eng.*, **19**(3), 393-408

IS 1608:2005 (2005), Indian Standard- Metallic Materials - Tensile Testing at Ambient Temperature; Bureau of Indian Standards, New Delhi, India, 1608–2005.

IS 800:2007 (2007), Indian Standard Code of Practice for General Construction in Steel; Bureau of Indian Standards, New Delhi, India.

IS 801:2010 (2010), Code of Practice for Use of Cold-Formed Light Gauge Steel Structural Members in General Building Construction, Bureau of Indian Standards, New Delhi, India.

Kumar, N. and Sahoo, D.R. (2016), "Optimization of lip length and aspect ratio of thin channel sections under minor axes bending", *Thin-Wall. Struct.*, **100**, 158-169.

Kumar, G.A. and Sukumar, S. (2014), "A Simplified method for calculating warping constant for lipped I-beam with Trapezoidal corrugation in web", *J. Struct. Eng. Madras*, **40**(6), 546-557.

Martins, C.H., Ferreira, F.P.V., Rossi, A. and Trentini, E.V.W. (2017), "Numerical analysis of physical and geometrical imperfections in cellular beams", *Open J. Civil Eng.*, **7**, 116-129.

Saleh, A., Zahrai, S.M. and Seyed, R.M. (2016), "Experimental study on innovative tubular web RBS connections in steel MRFs with typical shallow beams", *Struct. Eng. Mech., Int. J.*, **57(**5), 785-808.

Serror, M.H., Soliman, E.G. and Hassan, A.F. (2017), "Numerical study on the rotation capacity of CFRP strengthened cold formed steel beams", *Steel Compos. Struct., Int. J.*, **23**(4), 385-397.

Soliman, M.S., Abu-Sena, A.B.B., Darwish, E.E.D. and Saleh, M.S.R. (2013), "Resistance of cold-formed steel sections to combined bending and web crippling", *Ain Shams Eng. J.*, **4**(3), 435-453.

Valsa Ipe, T., Sharada Bai, H., Manjulavani, K. and Iqbal, M.M.Z. (2013), "Flexural behavior of cold-formed steel-concrete composite beams", *Steel Compos. Struct., Int. J.*, **14**(2), 105-120.

Zhou, W. and Jiang, L. (2017), "Distortional buckling of cold-formed lipped channel columns subjected to axial compression", *Steel Compos. Struct., Int. J.*, **23**(3), 331-338.